第 48 卷 第 13 期/2021 年 7 月/中国激光 研究论文

中国激光

基于 a 切 Er，Yb：$YAl_3(BO_3)_4$ 晶体被动调 Q 微片激光器

查松青[1,2]，陈雨金[2*]，邓鸣瑶[2,4]，林炎富[2]，李丙轩[2]，邹宇琦[3]，廖文斌[2]，林长浪[2]，张戈[2**]

[1]福州大学化学学院，福建 福州 351100；

[2]中国科学院福建物质结构研究所，福建 福州 351100；

[3]中国科学院上海硅酸盐研究所，上海 200000；

[4]福建师范大学化学与材料学院，福建 福州 351100

摘要 报道了基于 a 切 Er，Yb：$YAl_3(BO_3)_4$ 晶体的被动调 Q 微片激光器的性能。使用波长为 976 nm 的光纤耦合半导体二极管作为端面抽运光源，使用初始透过率为 96% 的 Co^{2+}：$MgAl_2O_4$ 晶体作为可饱和吸收体，耦合输出镜在 1500～1600 nm 波段范围的透过率为 2.5 %，整个微片激光器的腔长为 2.7 mm。在注入功率为 7.2 W 时，激光器成功得到了发射波长为 1530 nm、重复频率为 127 kHz 的稳定线性偏振的脉冲输出，对应的脉冲能量和脉冲宽度分别为 1.8 μJ 和 12 ns。

关键词 大气光学；a 切 Er，Yb：$YAl_3(BO_3)_4$ 晶体；Co^{2+}：$MgAl_2O_4$ 晶体；被动调 Q；微片激光器；线性偏振

中图分类号 O437 **文献标志码** A **doi**：10.3788/CJL202148.1301004

1 引 言

近年来由于无人驾驶技术的快速发展，车载雷达作为一项关键性技术引起了广泛的关注；其中激光雷达作为一种重要的雷达系统，也取得了很好的发展[1-3]。相对人眼安全的 1.5 μm 激光处于大气传输窗口，对空气有很好的穿透性而且容易被 Ge 和 InGaAs 这类探测器识别，所以 1.5 μm 激光雷达在车载方面有很好的应用前景[4-6]。考虑到车载雷达特殊的应用场景和复杂的工作环境，投入应用的激光雷达不仅要具备很好的脉冲性能（高重复频率、窄脉冲宽度、高脉冲能量），同时还要兼顾整个装置的稳定性、便携性以及生产成本。

微片激光器是以结构紧凑、稳定性强为特点的一种新型固态激光器。高度集成化的特性使得微片激光器便于工业化批量生产，器件生产成本比较低，所以微片激光器在工业生产上具备很大的潜力。此外，极短的腔长是微片激光器的另一大特点，结合被动调 Q 很容易实现持续时间极短的脉冲输出[7]。综合以上因素，被动调 Q 微片激光器是一种开发车载激光雷达的极佳方案。

目前市场上商用化的 1.5 μm 激光器使用的增益介质主要是 Er，Yb：glass。但是 Er，Yb：glass 受限于自身低的热导率（0.8 $W \cdot m^{-1} \cdot K^{-1}$）和低的热损伤阈值，这类激光器连续输出的最大功率仅为几百个毫瓦[6,8]。目前有很多关于基于不同可饱和吸收体的 Er，Yb：glass 被动调 Q 微片激光器的报道[如 Co^{2+}：$MgAl_2O_4$ 晶体[9]，Co^{2+}：Zn 晶体[10]以及半导体可饱和吸收镜（SESAM）[11-12]]，但这类激光器实现的重复频率一般不足 30 kHz，能量不超过 15 μJ，脉冲宽度约为 10 ns。为了得到更好性能的 1.5 μm 激光，近期有大量的研究集中在 Er/Yb 共掺的晶体上，如硼酸盐晶体[Er，Yb：$RAl_3(BO_3)_4$，R = Y，Gd 和 Lu]、硅酸盐晶体（Er，Yb：$Lu_2Si_2O_7$，Er，

收稿日期：2020-11-23；**修回日期**：2020-12-19；**录用日期**：2021-01-18

基金项目：国家自然科学基金（61875199，61975208）、中国科学院先导研究项目（XDB20000000）、福建省科学基金（2019J02015）、中国科学院科技网络服务项目（KFJ-STS-QYZX-069）、科技部重点研发专项（2018YFB2201101）

通信作者：*cyj@fjirsm.ac.cn；**zhg@fjirsm.ac.cn

Yb∶$Ca_3NbGa_3Si_2O_{14}$)、Er,Yb∶YAG 晶体、Er,Yb∶YVO_4 晶体等。表 1 整理了各类晶体中最具有代表性的晶体对应的连续激光实验参数。可以发现 Er,Yb∶YAB 激光器可以实现的最高输出功率(2 W)和转化效率(39.8%)要明显高于其他 Er/Yb 共掺晶体,这是因为 Er,Yb∶YAB 晶体具有极高的能量传递效率和高的热导率以及弱的上转化效应。因此 Er,Yb∶YAB 晶体被认为是 1.5 μm 波段激光增益介质的最佳选择。目前有很多关于 c 切 Er,Yb∶YAB 晶体被动调 Q 的报道[13],如最早期的平凹腔激光器[14]、热键合晶体的平凹腔激光器[15]、微片激光器[16-18]等,但这类激光器能够得到的脉冲都不是线性偏振的脉冲,能够实现的重复频率约为 100 kHz,脉冲宽度为 1~200 ns,能量不超过 10 μJ。本文报道了 a 切 Er,Yb∶YAB 晶体的被动调 Q 激光器的性能,成功得到了发射波长为 1530 nm、最大重复频率为 127 kHz 的稳定线性偏振的脉冲输出,对应的脉冲宽度和脉冲能量分别为 12 ns 和 1.8 μJ。

表 1 在连续激光实验中各类代表性晶体对应的转化效率和最大输出功率

Table 1 Conversion efficiency and maximum output power of various representative crystals in continuous laser experiments

Host crystal	Representative crystal	Pump wavelength / nm	Laser wavelength / nm	Conversion efficiency /%	Pump power /W	Maximum output power /W	Ref. No
Borate	Er,Yb∶$YAl_3(BO_3)_4$	976	1550	39.80	7.20 (incident power)	2.00	[16]
Silicate	Er, Yb∶$Lu_2Si_2O_7$	976	1564	20.00	5.50 (absorbable power)	0.94	[19]
Tungstate	Er, Yb∶$KY(WO_4)_2$	980	1590	1.66	6.50 (absorbable power)	0.08	[20]
Other	Er, Yb∶YAG	965	1645	7.00	0.45 (absorbable power)	0.03	[21]
	Er, Yb∶YVO_4	980	1604	5.40	2.25 (absorbable power)	0.13	[22]

2 a 切 Er, Yb∶YAB 晶体

Er,Yb∶YAB 晶体属于光学单轴晶,有 $\sigma(E\perp c)$ 和 $\pi(E/\!/c)$ 两个偏振吸收方向(光轴方向平行于 c 轴)。Er,Yb∶YAB 晶体具体的光学参数在先前的工作中已经被报道[23-24],其在 σ 偏振方向的吸收和发射系数远大于 π 方向的系数,所以 a 切的 Er,Yb∶YAB 晶体用作激光器的增益介质可以获得 σ 方向线性偏振的激光输出。

Er,Yb∶YAB 晶体属于硼酸盐晶体,具有很好的化学稳定性和高的机械强度,相对玻璃拥有更高的热导率,沿着 a 轴和 c 轴方向的热导率分别为 7 $W\cdot m^{-1}\cdot K^{-1}$ 和 6 $W\cdot m^{-1}\cdot K^{-1}$[25]。所以 Er,Yb∶YAB 晶体作为激光器的增益介质可以承受更高的注入功率,实现更强的脉冲输出。Er,Yb∶YAB 晶体的能级结构和激光运转机制如图 1 所示。Er,Yb∶YAB 晶体在能级 $^4I_{13/2}$ 和 $^4I_{11/2}$ 上的荧光寿命较短,分别为 0.33 ms 和 80 ns;然而传统的 Er,Yb∶glass 在 $^4I_{13/2}$ 和 $^4I_{11/2}$ 上的荧光寿命分别为 8~9 ms 和 2~3 μs[5]。Er,Yb∶YAB 晶体较短的荧光寿命有助于实现高重复频率的脉冲运转;此外,短的荧光寿命会抑制 Er 离子的上转化过程[23,26]。所以将 Er,Yb∶YAB 晶体用作被动调 Q 的增益介质有利于实现高重复频率、高转化效率的脉冲输出。

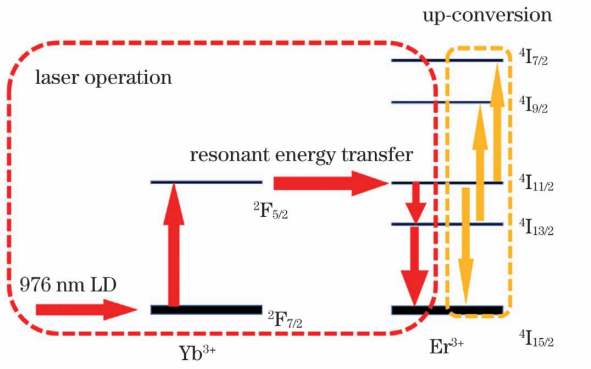

图 1 Er,Yb∶YAB 晶体的能级结构激光运转机制简图

Fig. 1 Diagram of laser operating mechanism of energy level structure in Er, Yb∶YAB crystal

3 实验装置

实验使用尺寸为 3 mm×3 mm×1.5 mm 的 a 切 Er(原子数分数为 1.5%),Yb(原子数分数为 12%):YAB 晶体作为激光器增益介质;使用尺寸为 3 mm×3 mm×1.2 mm 的掺钴尖晶石(Co^{2+}∶$MgAl_2O_4$ 晶体)作为被动调 Q 的可饱和吸收体。

使用紫外可见近红外分光光度计(Lambda 950, PerkinElmer)测量掺钴尖晶石的透过率光谱[图 2(a)],其在 1.5 μm 波段的初始透过率 T_0 约为 96%。Co^{2+} : $MgAl_2O_4$ 晶体用作可饱和吸收体的可饱和吸收特性在先前的工作中已经被报道[27]。实验使用的注入镜 IM 镀有对 976 nm 抽运光的增透膜(透过率 $T>90\%$)和对 1500～1600 nm 激光的高反膜(反射率 $R>99.9\%$);输出镜 OC 在 1500～1600 nm 范围内的透过率为 2.5%。

实验装置如图 2(b)所示,将发射波长为 976 nm 的光纤耦合半导体二极管作为端面泵浦的光源。光纤的芯径为 105 μm,数值孔径为 0.22。利用两个焦距为 40 mm 的透镜,将泵浦光束聚焦为束腰半径为 60 μm 的光束打在激光晶体上。微片腔的架构如图 2 中的结构图所示,激光器的输入镜 IM 和输出镜 OC 分别镀在两个蓝宝石晶体上,然后将 IM 和 OC 分别贴在激光晶体和尖晶石晶体的两个外侧表面,共同构成了整个激光器谐振腔,腔长为 2.7 mm。两片蓝宝石在激光器中起到了热沉的作用,因此整个微片激光器的散热方式为端面散热。将整个谐振腔放置在铜块内,通光方向的两端用两个铜片夹紧,铜片上有半径为 0.75 mm 的小孔以使泵浦光和激光通过。通过水冷将整个铜块温度控制在 19 ℃。

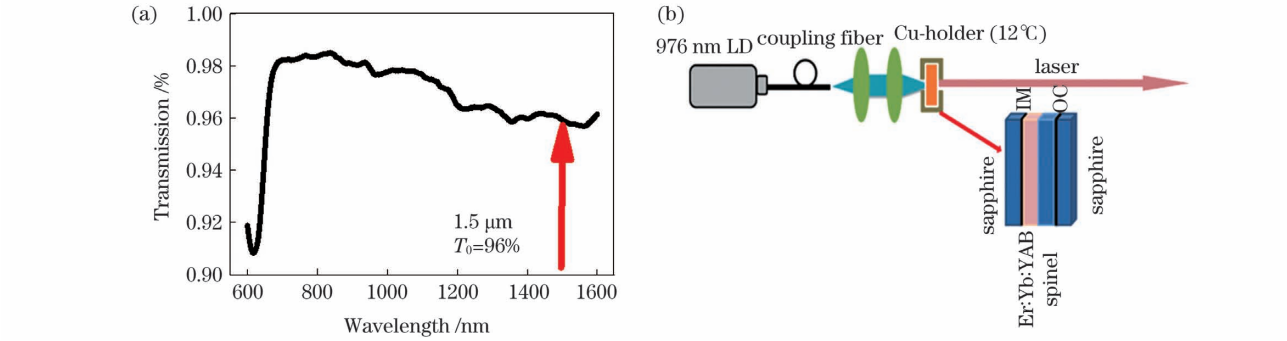

图 2　Co^{2+} : $MgAl_2O_4$ 晶体的透过率光谱,以及 a 切 Er,Yb : YAB 被动调 Q 微片激光器的架构。(a) Co^{2+} : $MgAl_2O_4$ 晶体的透过率光谱;(b)a 切 Er,Yb : YAB 被动调 Q 微片激光器的架构

Fig. 2　Transmission spectrum of Co^{2+} : $MgAl_2O_4$ crystal, and experimental setup for passively Q-switched a-cut Er, Yb : YAB microchip laser. (a) Transmission spectrum of Co^{2+} : $MgAl_2O_4$ crystal; (b) experimental setup for passively Q-switched a-cut Er, Yb : YAB microchip laser

4　实验结果与分析

在发射波长为 976 nm 的半导体二极管连续抽运作用下,微片激光器成功实现了脉冲输出。实验使用 Thorlab 公司生产的 S314C 功率探头连接 PM100D 功率显示器,对激光器的输出功率进行监测。采用上升时间为 225 ps 的快速光电探测器接收产生的脉冲激光,并使用带宽为 1 GHz 的数字示波器显示各个阶段的波形,得到的实验结果如图 3 和图 4 所示。

由图 3 可知,微片激光器的阈值为 4 W。当注入功率从 4 W增大到 6 W时,激光器的平均输出功

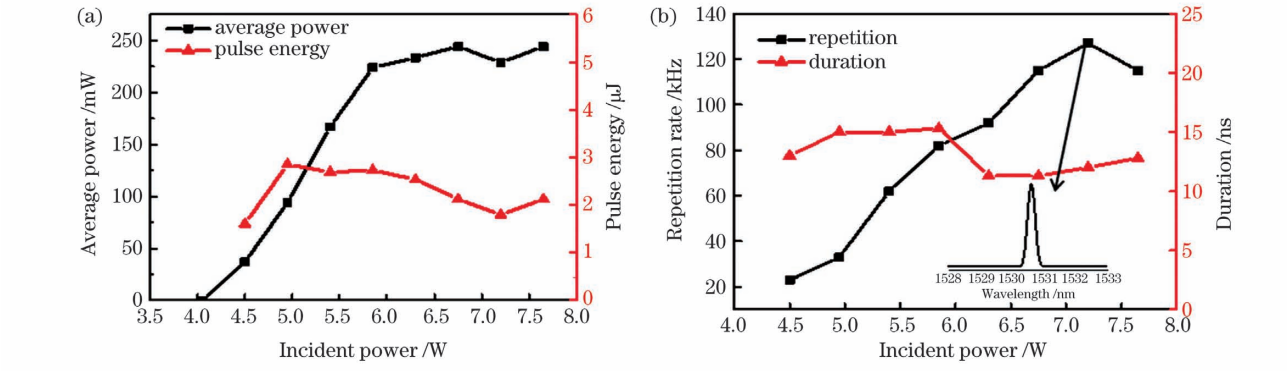

图 3　微片激光器的实验性能。(a)平均输出功率和单脉冲能量;(b)重复频率和脉冲宽度

Fig. 3　Experimental performance of microchip laser. (a) Average output power and single pulse energy; (b) repetition rate and pulse duration

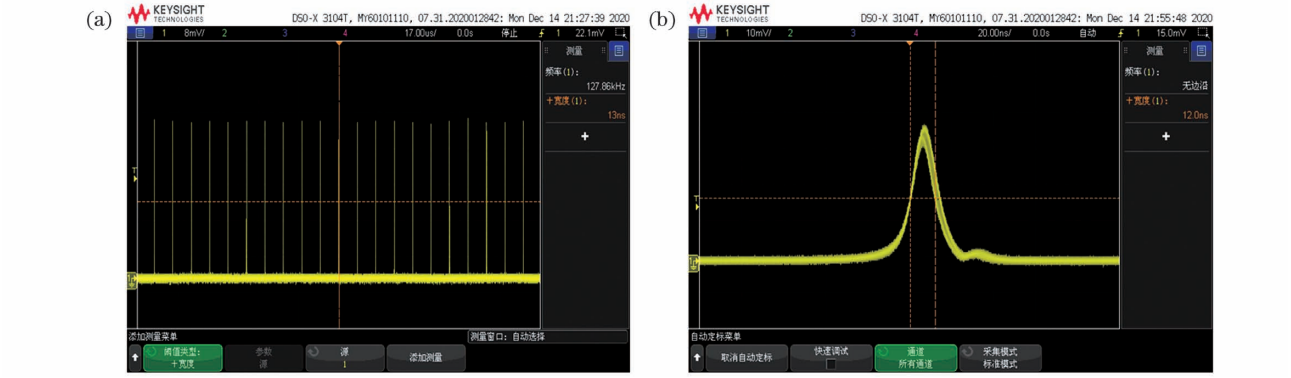

图 4　注入功率 7.2 W 时示波器记录的结果。(a)脉冲序列和脉冲重复频率;(b)单个脉冲波形及脉冲宽度

Fig. 4　Results recorded by oscilloscope for incident power of 7.2 W. (a) Pulse train and pulse repetition rate; (b) single pulse profile and pulse duration

率不断增大;然而,当注入功率继续增大时,输出功率不会得到明显提高。这是因为在高功率泵浦抽运作用下,微片激光器的热效应会变强,使得热透镜的焦距变短,导致激光器模式匹配变差。因此,注入功率超过 6 W 后继续增大注入功率并不能显著增大激光晶体的增益,导致输出功率不会得到明显的提升。脉冲的重复频率随着注入功率的增大而增大,超过 7.2 W 时会突然下降。这是因为高阶的激光模式被激发出来,激光的光斑面积会增大,单位面积上的增益减小。为了避免激光晶体的热胀裂,实验中的注入功率始终保持在 8 W 以下。

实验获得的最大输出功率为 275 mW,大于先前 Er,Yb∶glass 的输出功率 150 mW[5];实验获得的最大重复频率为 127 kHz,也大于先前 Er,Yb∶glass 实现的被动调 Q 的重复频率(不足 30 kHz)。正如前文分析,Er,Yb∶YAB 晶体具有更好的热导能力和较大的机械强度,同时还具备很短的荧光寿命,所以使用 Er,Yb∶YAB 晶体作为增益介质的激光器有助于实现高重复频率的脉冲输出。使用 A. P. E 公司的 waveScan Laserspectrometer 光谱探测器对 127 kHz 脉冲的光谱进行探测,得到的光谱如图 3(b)中插图所示;脉冲的发射波长约为 1530 nm,这与先前报道的 Er,Yb∶YAB 晶体的发射光谱一致[23-24]。脉冲序列如图 4(a)所示,可以发现整个脉冲序列非常稳定,没有观测到脉冲波动的现象。单个脉冲的轮廓如图 4(b)所示,脉冲半峰全宽为 12 ns,脉冲宽度明显要比平凹腔激光器[14-15]的脉冲宽度(265 ns 和 315 ns)更窄。这是因为微片激光器的腔长短,有利于调 Q 脉冲的快速运转。

微片激光器的脉冲能量始终维持在 2 μJ 左右,脉冲宽度稳定在 13 ns。实验中的脉冲宽度和脉冲能量受抽运功率的影响很小,这一结果符合先前 Keller 对 1.5 μm 被动调 Q 微片激光器脉冲参数的理论仿真[12, 28]。由于 a 切的 Er,Yb∶YAB 晶体中 σ 偏振方向的发射系数大于 π 方向的发射系数,所以该激光器会获得 σ 方向的线性偏振的脉冲输出。使用格兰棱镜对脉冲的偏振性进行了检测,结果如图 5 所示,脉冲偏振的消光比约为 44∶1。使用 thorlabs beam 7.0 光束分析仪对 127 kHz 脉冲的形貌进行探测,得到光斑形貌的 2D 和 3D 图像如图 5(b)所示,可以看出,激光器输出的光斑椭圆度较好,能量分布均匀。

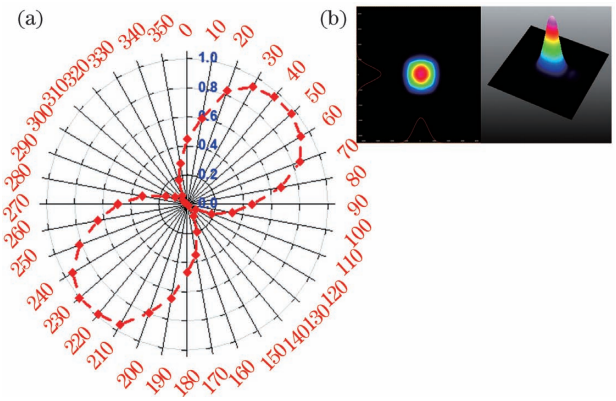

图 5　脉冲激光的偏振检测结果,以及脉冲输出光斑的 2D 和 3D 图像。(a)脉冲激光的偏振检测结果;(b)脉冲输出光斑的 2D 和 3D 图像

Fig. 5　Test result of pulse laser polarization, and 2D and 3D images of pulse output spots. (a) Test result of pulse laser polarization; (b) 2D and 3D images of pulse output spots

5　结　　论

首次报道了基于 a 切 Er,Yb∶YAB 晶体被动

调 Q 激光器的性能。实验采用初始透过率为 96% 的 Co^{2+} ∶ $MgAl_2O_4$ 晶体作为调 Q 可饱和吸收体，搭建了腔长为 2.7 mm 的微片激光器。在注入功率达到 7.2 W 时，成功实现了最大重复频率为 127 kHz 的稳定的脉冲输出，对应的脉冲宽度为 12 ns，脉冲能量为 1.8 μJ。由于 a 切 Er，Yb ∶ YAB 晶体 σ 偏振方向的吸收系数远大于 π 方向的吸收系数，微片激光器获得了 σ 方向的线性偏振的激光输出。该实验为实现高重复频率线性偏振的 1.5 μm 的脉冲输出提供了可靠方案。

参 考 文 献

[1] Chen S J, Zhu Z C, Zhang Y H, et al. Extrinsic calibration for lidar and stereo vision using 3D feature points[J]. Laser & Optoelectronics Progress, 2020, 57(3): 030102.
陈少杰, 朱振才, 张永合, 等. 基于 3D 特征点的激光雷达与立体视觉配准方法[J]. 激光与光电子学进展, 2020, 57(3): 030102.

[2] Guo Y D, Wang X K, Su D P, et al. Building orthogonal boundary extraction for airborne LiDAR based on directional prediction regularization [J]. Laser & Optoelectronics Progress, 2020, 57(6): 062801.
郭亚栋, 王贤昆, 宿殿鹏, 等. 基于方向预测规则化的机载激光雷达建筑物正交轮廓线提取[J]. 激光与光电子学进展, 2020, 57(6): 062801.

[3] Yang Y, Li H N. Automatic power line extraction method based on airborne LiDAR point cloud data [J]. Laser & Optoelectronics Progress, 2020, 57(9): 090102.
杨业, 李宏宁. 基于机载 LiDAR 点云数据的电力线自动提取方法[J]. 激光与光电子学进展, 2020, 57(9): 090102.

[4] Myers M J, Myers J D, Sarracino J T, et al. LIBS system with compact fiber spectrometer, head mounted spectra display and hand held eye-safe erbium glass laser Gun [J]. Proceedings of SPIE, 2010, 7578: 75782G.

[5] Karlsson G, Laurell F, Tellefsen J, et al. Development and characterization of Yb-Er laser glass for high average power laser diode pumping [J]. Applied Physics B, 2002, 75(1): 41-46.

[6] Laporta P, Taccheo S, Longhi S, et al. Erbium-ytterbium microlasers: optical properties and lasing characteristics[J]. Optical Materials, 1999, 11(2/3): 269-288.

[7] Zayhowski J J. Microchip lasers [J]. Optical Materials, 1999, 11(2/3): 255-267.

[8] Taccheo S, Sorbello G, Laporta P, et al. 230-mW diode-pumped single-frequency Er ∶ Yb laser at 1.5 μm [J]. IEEE Photonics Technology Letters, 2001, 13(1): 19-21.

[9] Karlsson G, Pasiskevicius V, Laurell F, et al. Diode-pumped Er-Yb ∶ glass laser passively Q switched by use of Co^{2+} ∶ $MgAl_2O_4$ as a saturable absorber [J]. Applied Optics, 2000, 39(33): 6188-6192.

[10] Kisel' V É, Shcherbitsky V G, Kuleshov N V, et al. Spectral kinetic properties and lasing characteristics of diode-pumped Cr^{2+} : ZnSe single crystals[J]. Optics and Spectroscopy, 2005, 99(4): 663-667.

[11] Fluck R, Häring R, Paschotta R, et al. Eyesafe pulsed microchip laser using semiconductor saturable absorber mirrors[J]. Applied Physics Letters, 1998, 72(25): 3273-3275.

[12] Häring R, Paschotta R, Fluck R, et al. Passively Q-switched microchip laser at 15 μm[J]. Journal of the Optical Society of America B, 2001, 18(12): 1805-1812.

[13] Chen Y J, Lin Y F, Huang J H, et al. Research progress in 1550-nm all-solid-state lasers based on Er^{3+}-doped crystals [J]. Chinese Journal of Lasers, 2020, 47(5): 0500018.
陈雨金, 林炎富, 黄建华, 等. 基于掺 Er^{3+} 晶体的 1550 nm 波段全固态激光研究进展[J]. 中国激光, 2020, 47(5): 0500018.

[14] Chen Y J, Lin Y F, Zou Y Q, et al. Diode-pumped 1.5–1.6 μm laser operation in Er^{3+} doped $YbAl_3(BO_3)_4$ microchip[J]. Optics Express, 2014, 22(11): 13969-13974.

[15] Chen Y J, Lin Y F, Huang J H, et al. Efficient continuous-wave and passively Q-switched pulse laser operations in a diffusion-bonded sapphire/Er ∶ Yb ∶ $YAl_3(BO_3)_4$/sapphire composite crystal around 1.55 μm[J]. Optics Express, 2018, 26(1): 419-427.

[16] Chen Y J, Lin Y F, Yang Z M, et al. Eye-safe 1.55 μm Er ∶ Yb ∶ $YAl_3(BO_3)_4$ microchip laser[J]. OSA Continuum, 2019, 2(1): 142-150.

[17] Chen Y J, Lin Y F, Huang J H, et al. Enhanced performances of diode-pumped sapphire/Er^{3+} ∶ Yb^{3+} ∶ $LuAl_3(BO_3)_4$/sapphire micro-laser at 1.5–1.6 μm[J]. Optics Express, 2015, 23(9): 12401-12406.

[18] Kisel V E, Gorbachenya K N, Yasukevich A S, et al. Passively Q-switched microchip Er, Yb ∶ $YAl_3(BO_3)_4$ diode-pumped laser[J]. Optics Letters, 2012, 37(13): 2745-2747.

[19] Huang J H, Chen Y J, Lin Y F, et al. 940 mW 1564 nm multi-longitudinal-mode and 440 mW 1537 nm single-longitudinal-mode continuous-wave

Er∶Yb∶$Lu_2Si_2O_7$ microchip lasers [J]. Optics Letters, 2018, 43(8): 1643-1646.

[20] Bjurshagen S, Brynolfsson P, Pasiskevicius V, et al. Crystal growth, spectroscopic characterization, and eye-safe laser operation of erbium-and ytterbium-codoped $KLu(WO_4)_2$ [J]. Applied Optics, 2008, 47(5): 656-665.

[21] Schweizer T, Jensen T, Heumann E, et al. Spectroscopic properties and diode pumped 1.6 μm laser performance in Yb-codoped Er∶$Y_3Al_5O_{12}$ and Er∶Y_2SiO_5 [J]. Optics Communications, 1995, 118(5/6): 557-561.

[22] Tolstik N A, Troshin A E, Kurilchik S V, et al. Spectroscopy, continuous-wave and *Q*-switched diode-pumped laser operation of Er^{3+}, Yb^{3+}∶YVO_4 crystal[J]. Applied Physics B, 2007, 86(2): 275-278.

[23] Tolstik N A, Kisel V E, Kuleshov N V, et al. Er, Yb∶$YAl_3(BO_3)_4$: efficient 1.5 μm laser crystal[J]. Applied Physics B, 2009, 97(2): 357-362.

[24] You W X, Lin Y F, Chen Y J, et al. Growth and spectroscopic properties of Er^{3+} single doped and Er^{3+}-Yb^{3+} co-doped $YAl_3(BO_3)_4$ crystals [J]. Journal of Crystal Growth, 2004, 270(3/4): 481-485.

[25] Tolstik N A, Huber G, Maltsev V V, et al. Excited state absorption, energy levels, and thermal conductivity of Er^{3+}∶YAB [J]. Applied Physics B, 2008, 92(4): 567-571.

[26] Tolstik N A, Kurilchik S V, Kisel V E, et al. Efficient 1 W continuous-wave diode-pumped Er, Yb∶$YAl_3(BO_3)_4$ laser [J]. Optics Letters, 2007, 32(22): 3233-3235.

[27] Yumashev K V, Denisov I A, Posnov N N, et al. Nonlinear absorption properties of Co^{2+}∶$MgAl_2O_4$ crystal[J]. Applied Physics B, 2000, 70(2): 179-184.

[28] Spühler G J, Paschotta R, Fluck R, et al. Experimentally confirmed design guidelines for passively *Q*-switched microchip lasers using semiconductor saturable absorbers: errata [J]. Journal of the Optical Society of America B, 2001, 18(6): 886.

Passively *Q*-Switched *a*-Cut Er, Yb∶$YAl_3(BO_3)_4$ Microchip Laser

Zha Songqing[1,2], Chen Yujin[2*], Deng Mingyao[2,4], Lin Yanfu[2], Li Bingxuan[2], Zou Yuqi[3], Liao Wenbin[2], Lin Zhanglang[2], Zhang Ge[2**]

[1] *School of Chemistry, Fuzhou University, Fuzhou, Fujian* 351100, *China*;

[2] *Fujian Institute of Research on the Structure of Matter, Chinese Academy of Sciences, Fuzhou, Fujian* 351100, *China*;

[3] *Shanghai Institute of Ceramics, Chinese Academy of Science, Shanghai* 200000;

[4] *College of Chemistry and Materials Science, Fujian Normal University, Fuzhou, Fujian* 351100, *China*

Abstract

Objective With their high sensitivity to Ge and InGaAs and excellent transparency in the atmosphere, eye-safe lasers emitting in the 1.5–1.6 μm spectral range have great application prospects in the lidar, rangefinder, and three-dimensional imaging. Vehicular lidars operating at 1.5 μm have attracted wide attention in the recent development of unmanned aerial vehicles (UAVs). Therefore, high-performance 1.5-μm lasers with high repetition rate, high pulse energy, and narrow pulse duration are commercially valuable. Passively *Q*-switched lasers operating at 1.5 μm in different gain media, such as Er^{3+}/Yb^{3+} co-doped borated crystals and phosphate, have been often reported. Owing to their high thermal conductivity, high $Yb^{3+} \rightarrow Er^{3+}$ energy-transfer efficiency, and weak up-conversion loss, Er, Yb∶YAB crystals are considered as an excellent 1.5 μm laser material. However, all previous reports on Er, Yb∶YAB lasers have employed *c*-cut Er, Yb∶YAB crystals. This paper reports a passively *Q*-switched microchip laser with an *a*-cut Er, Yb∶YAB crystal.

Methods This paper explores a passively *Q*-switched microchip laser with an *a*-cut Er, Yb∶YAB laser crystal as the gain medium. The experimental setup is shown in Fig. 2(b). The detailed performance of a laser with an *a*-cut Er (atomic fraction of 1.5%)∶Yb (atomic fraction of 12%)∶YAB crystal was reported in our previous work. In the present experiment, a Co^{2+}∶$MgAl_2O_4$ crystal with an initial transmission of 96% at 1.5 μm was employed as the saturable absorber. An input mirror and an output coupler were separately coated on the surfaces of two sapphire crystals, which acted as heat sinks in the microchip laser. The input-mirror material was antireflective in the

800–1000 nm range and reflected 99.8% of the light in the 1500–1600 nm range. Meanwhile, the output coupler transmitted 2.5% of the light in the 1500–1600 nm range. The input mirror and output coupler were tightly attached to the surfaces of the Er∶Yb∶YAB and Co^{2+}∶$MgAl_2O_4$ crystal, respectively. The resonator length was 2.7 mm. The pump source was a 976-nm diode laser with a central wavelength of 975.5 nm, a core diameter of 105 μm, and a numerical aperture of 0.22. After passing the lens assembly, the pump beam was focused into the laser crystal (with approximate radius of 60 μm). The microchip laser was maintained at 19 ℃ by water-cooling.

Results and Discussions Pumped by the 976 nm diode laser, the microchip laser successfully generated 1.5-μm pulses. The output power of the laser was measured by a PM 100D power meter with an S314C thermal power head. The pulse profile was recorded by an InGaAs photodiode connected to a digital oscilloscope with a 1.0-GHz bandwidth, and the laser spectrum was recorded by a wavescan laser-spectrometer. From the plotted dependence of average output power on the incident power (Fig. 3), the laser threshold was determined as 4 W. The average output power increased as the incident pumped power increased from 4 to 6 W. At higher incident powers (> 6 W), the average output power was not obviously increased and bends appeared in the output characteristics. The average output power was maximized at 275 mW. The repetition rate increased with incident pump power, and was maximized at 127 kHz. The pulse train [Fig. 4(a)] was stable and the pulse-amplitude variations and time jittering remained at 5%. The pulse duration [Fig. 4(b)] was 12 ns, narrower than that in previous reports. The laser wavelength was 1530 nm, consistent with previously reported emission spectra of Er, Yb∶YAB crystals. The pulse energy and pulse duration remained at approximately 2 μJ and 13 ns, respectively. As the Er∶Yb∶YAB crystal is optically uniaxial, it was characterized for two principal light polarizations, $E//c(\pi)$ and $E\perp c(\sigma)$ (in which the optical axis is parallel and perpendicular to the c axis, respectively). The emission coefficient was much higher in σ-polarization than that in π-polarization, implying linear polarization of the pulses generated from the a-cut Er, Yb∶YAB microchip laser. In pulse-polarization tests (Fig. 5), the extinction ratio of the pulse laser was 44∶1. The spatial profile of the output beam presented high ellipticity and an even energy distribution. Therefore, a high-repetition-rate linear polarization laser was successfully fabricated from the microchip.

Conclusions This paper reports a microchip laser based on an a-cut Er, Yb∶YAB crystal. A Co^{2+}∶$MgAl_2O_4$ crystal with an initial transmission of 96% was employed as the saturable absorber. The cavity length and maximum repetition rate of the microchip laser were 2.7 mm and 127 kHz, respectively, corresponding to the pulse energy and duration of 1.8 μJ and 12 ns, respectively. The emission coefficient was much larger in σ-polarization than that in π-polarization, indicating linear polarization of the pulse laser. In summary, a high-repetition-rate linearly polarized 1.5-μm pulse laser was fabricated by a simple and reliable method.

Key words atmospheric optics; a-cut Er, Yb∶$YAl_3(BO_3)_4$ crystal; Co^{2+}∶$MgAl_2O_4$ crystal; passive Q-switching; microchip laser; linear polarization

OCIS codes 140.3540; 140.3580; 140.3945; 140.3948